

Application of Haptic Interface for Finger Exercise

Uroš Mali, Nika Goljar, and Marko Munih, *Member, IEEE*

Abstract—A haptic device with two active degrees-of-freedom and a tendon-driven transmission system was designed, later on constructed, and submitted to testing. It was embodied as a light-weight mechanism with a small workspace that wraps the finger workspace and can generate forces up to 10 N suitable for finger exercise. The control loop and the user application were implemented on a personal computer in the Microsoft Windows environment. Along with the device, application covering several different experiment types was developed. The system was evaluated in a group of stroke patients during a one-month period of therapy. Results for two types of experiments are presented. The progress of the patient affected hand side was found to be greater than for the one nonaffected, however, the mean values of the relevant parameters on the nonaffected side of patients are higher than those for the affected side. Results were compared to the motor component of functional independence measure (M-FIM) measured clinical scale.

Index Terms—finger exercise, force control, haptic interface, virtual rehabilitation.

I. INTRODUCTION

FINGER movement control and grasping are among the most meaningful and precious human motion activities [1]–[3]. This is reflected in many daily activities first connected to the motion ability of fingers, e.g., grasping and picking up and, secondly, connected to the grip-force control, e.g., holding objects and pushing buttons. Besides, a reliable and stable grip, coordination of finger movement and force is also required [4]–[6]. A good interconnection between the central nervous system (CNS) and the muscles is necessary for coordination of motion and force [5], [7]. Subjects with damaged CNS or those who have suffered hand and finger injuries of the skeletal or neuromuscular system, exhibit limited hand functionality, which hampers the activities of everyday life. A hand functionality assessment has been applied as a basis for prescription of therapy in diagnostics and rehabilitation.

Hand functionality can be defined as an ability to grasp objects and to manipulate same [4], functionality depending upon finger and wrist ranges of motion, upon grasping forces, and the sensory-motor capacity of subject. Usually, functionality is presented as a quantitative estimate, which can vary with subjective criteria and the experience of the therapist. Based on such estimate, small changes caused by the progression of a disease or

effectiveness of therapy are rarely evidenced and taken consideration of. Computer-assisted methods can increase the accuracy and the objectivity of assessment while examination time and resources are reduced.

After injury or finger paralysis the rehabilitation process can be very long. Usually, treatment takes place at a clinic where an occupational therapist administers exercises according to a treatment program. Throughout the rehabilitation process, the therapist applies use of force to the injured finger to allow same to regain its strength and range of motion. Therefore, an interface that can imitate the exercises of therapist would be beneficial. The interface should have the ability of position and force control. Haptic devices, which can by definition generate a controlled force to a single finger, were selected as a suitable type of device for the application of finger exercise.

Virtual reality in connection with haptic interfaces has already been used for rehabilitation or hand assessment purposes [8]–[12]. Burdea has pointed out several advantages e.g., motivation, adaptability, heterogeneity, data analysis, reduced costs, and challenges of “virtual rehabilitation” [13], such as lack of computer skills on the part of therapist, lack of support infrastructure, expensive equipment, and patient safety concerns. It has been shown that virtual rehabilitation increases patient motivation for a longer period of time, thereby enhancing the effectiveness of therapy [11], [14], [12]. Appropriate methods in connection with virtual reality are different force or position tracking tasks [15], and tasks imitating the daily activities. Bardorfer *et al.* used a haptic device for an objective test to evaluate functional studies of the upper limbs in patients with neurological diseases [16]. The Fifth Framework Programme of the European Commission project GENTLE/s has taken a rapid prototyping approach to developing the technology for machine-mediated stroke rehabilitation [12]. Work was completed on a second-phase prototype based on a modified HapticMaster haptic interface by FCS Control Systems.

In contrast to the above, many research projects deal with devices measuring or assessing finger joint movement only [17]–[22]. None of these devices have applied force for finger movement. Authors wanted to extend the single measuring function further with a force-feedback function in a haptic device that can generate and provide force information, as well as fingertip position.

There are a few small, commercially-available haptic interfaces, such as PHANTOM by SensAble Technologies [23], [24], CyberGrasp by Immersion Corporation [25], and the Rutgers Masters II force-feedback glove [26], etc. Despite the variety of haptic devices available [27] there has so far existed no device that is especially well suited for finger exercise. The above-listed haptic devices either exhibit insufficient continuous output forces, or their workspaces have limited size. This paper presents a haptic interface for finger exercise

Manuscript received March 5, 2004; revised March 15, 2006; accepted March 25, 2006.

U. Mali and M. Munih are with the Laboratory of Robotics and Biomedical Engineering, Faculty of Electrical Engineering, University of Ljubljana, SI-1000 Ljubljana, Slovenia (e-mail: urosmali@robo.fe.uni-lj.si; marko@robo.fe.uni-lj.si).

N. Goljar is with the Institute for Rehabilitation, Republic of Slovenia, Linhartova 51, SI-1000 Ljubljana, Slovenia.

Digital Object Identifier 10.1109/TNSRE.2006.881535

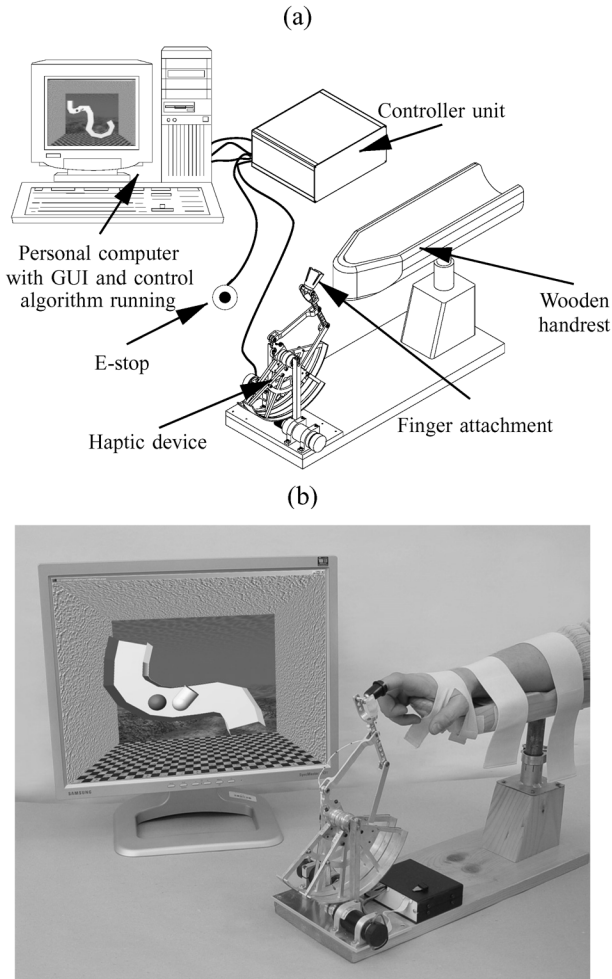


Fig. 1. (a) Haptic interface for finger exercise setup. Setup consists of a personal computer running a graphic user interface and control algorithm of a controller unit and a haptic device. (b) First prototype of the HIFE.

(HIFE) [28] during the rehabilitation process. Shown here are kinematic and dynamic models of the device and a method for estimating contact force between the finger and the device over the whole working range in the sagittal plane of the finger. Also provided are a description of the accompanying haptic interface components, and several pre-programmed exercises for fingers. Furthermore, application, experiment features, data analysis, and statistical analysis are presented. The system was evaluated in a group of stroke patients during a one-month period of therapy. Results of two types of experiments, and analytical observations thereon are given in present paper.

II. METHODS

A. Haptic Interface

The haptic interface consists of a personal computer, a controller unit, and a haptic device. The component setup and a prototype thereof are shown in Fig. 1. The haptic device is controlled by a personal computer through a custom-designed controller unit. The PC runs a control loop and provides visual feedback from the haptic device. Two data acquisition cards (Measurement Computing PCI-DDA08/12 and PCI-QUAD04)

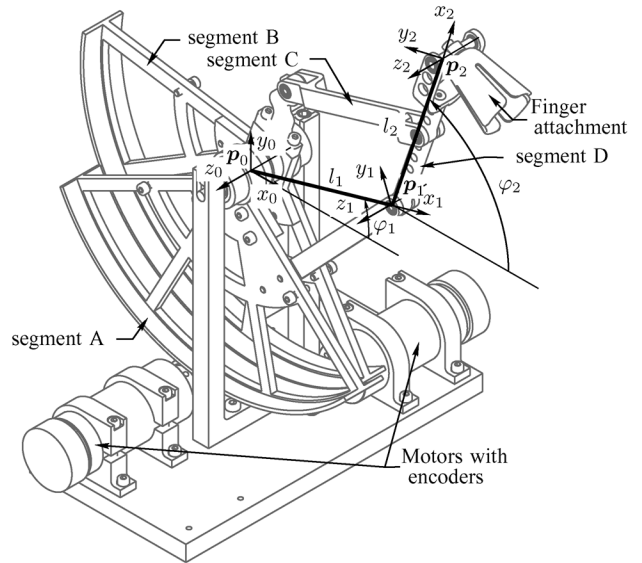


Fig. 2. Haptic device with back-drivable lightweight mechanism for finger exercise. Mechanism has two active DOF and two passive DOF at the finger attachment. It is actuated by two ironless-rotor brushed dc motors. This figure also presents the coordinate systems and the general notation applied for derivation of direct kinematic and dynamic model equations.

are connected to the personal computer PCI bus. The computer is connected to an external controller unit, which includes a real-time clock generator, a watchdog timer, power amplifiers for the motors, and several safety mechanisms, the formal external unit designed in-house.

Furthermore, to take full advantage of the input/output capability of the haptic interface, real-time and software requirements are set. The control application runs in real-time with strict timing constraints [29].

1) *Design of Haptic Device:* A haptic device was built with a back-drivable lightweight mechanism suitable for finger exercise during rehabilitation. The mechanism has two active degrees-of-freedom (DOF) and two passive DOF at the finger attachment. It is actuated by two ironless-rotor brushed direct current (dc) motors with linear current versus torque characteristic. Each motor is equipped with an optical position encoder with a resolution of 1024 pulses per revolution. The manipulator top position resolution reading is 0.05 mm or better. The haptic display design and the configuration thereof allow estimation of finger forces at the attachment point without using force/torque sensors. In order to obtain an appropriate workspace size, calculations for the human finger workspace range on the basis of known finger dimensions and range of motion were performed first. The anthropometric data on fingers used for the finger workspace size calculations were taken from [30]. The haptic device model sketch is shown in Fig. 2.

Along with the mechanism, an accurate dynamic model of the haptic device was also developed [28]. Model parameters were identified on the basis of the device to attain model responses similar to those according to the actual system. The model is then used for estimating contact forces at the tip of the device, and for controlling required motor torques. Within the model, separate contributions were identified including Coriolis, centripetal, and gravity forces.

2) *Kinematic Model of Device*: On the basis of the kinematic data of the parallel mechanism and known values of joint angles of mechanism, the position of the manipulator end point \mathbf{p}_2 can be defined through direct kinematic equation

$$\mathbf{p}_2 = \mathbf{p} = \begin{bmatrix} p_x \\ p_y \end{bmatrix} = \begin{bmatrix} l_1 \cos \varphi_1 + l_2 \cos \varphi_2 \\ l_1 \sin \varphi_1 + l_2 \sin \varphi_2 \end{bmatrix} \quad (1)$$

where l_1, l_2, φ_1 , and φ_2 represent manipulator segment lengths and joint angles, respectively. Additionally, the inverse kinematics enables calculation of angles φ_1 and φ_2 of known position of finger support coordinates p_x and p_y . Further details can be found in [28].

To calculate the velocity of the finger support point \mathbf{p} of angular velocities of active joints, the analytical Jacobian matrix of manipulator must be defined. The analytical Jacobian of same is determined as follows:

$$\mathbf{J}_A(\varphi) = \begin{bmatrix} \frac{\partial p_x}{\partial \varphi_1} & \frac{\partial p_x}{\partial \varphi_2} \\ \frac{\partial p_y}{\partial \varphi_1} & \frac{\partial p_y}{\partial \varphi_2} \end{bmatrix} = \begin{bmatrix} -l_1 \sin \varphi_1 & -l_2 \sin \varphi_2 \\ l_1 \cos \varphi_1 & l_2 \cos \varphi_2 \end{bmatrix}. \quad (2)$$

Finger support velocity $\dot{\mathbf{p}}$ depends upon joint angular velocities $\dot{\varphi}$ as follows:

$$\dot{\mathbf{p}} = \mathbf{J}_A(\varphi)\dot{\varphi}. \quad (3)$$

Similarly, in static conditions and with a rigid-link manipulator, the Jacobian also defines a simple force-torque relationship between the end-effector and the actuators

$$\boldsymbol{\tau}_E = \mathbf{J}_A^T(\varphi)\mathbf{f} \quad (4)$$

where \mathbf{f} represents generalized forces exerted on the end-effector, $\boldsymbol{\tau}_E$ representing the generalized forces exerted by the actuators in the joints.

3) *Dynamic Model of Device*: A full manipulator dynamic model without contact force contribution is written using matrix notation:

$$\mathbf{M}(\varphi)\ddot{\varphi} + \mathbf{C}(\varphi, \dot{\varphi})\dot{\varphi} + \mathbf{F}(\dot{\varphi})\dot{\varphi} + \mathbf{G}(\varphi) = \boldsymbol{\tau} - \mathbf{J}_A^T(\varphi)\mathbf{f} \quad (5)$$

where \mathbf{M} represents inertia matrix, \mathbf{C} being matrix of Coriolis and centripetal contributions, \mathbf{F} representing viscous friction matrix, and \mathbf{G} meaning gravity vector [31]. The mechanical design procedure provided estimates of certain parameters, e.g., masses, moments of inertia, dimensions, and transmission ratios. On the other hand, there is another set of parameters, such as the friction of ball bearings or the elasticity of tendon wire, that were identified on the device itself. The final dynamic model includes all relevant contributions and only excludes those that can be neglected.

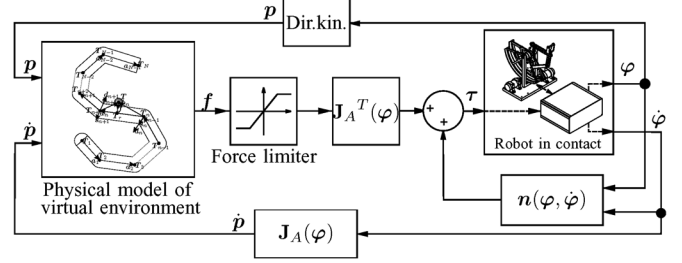


Fig. 3. Control scheme of the haptic interface in connection with a virtual environment.

B. Control Scheme

Fundamentally, haptic devices are mechanical manipulators—robots—they being active devices. Control of a device includes control in free movement and also control in contact with the environment. Thus, impedance or admittance control is suitable [23], [31]. Due to the back-drivable mechanism of HIFE, open loop impedance control was used. Inputs in the control scheme or the physical model of virtual environment are the position and the velocity of the mechanism tip, the output being a reference of the output force. The control scheme is depicted in Fig. 3.

From known position of the end point of manipulator, the physical model algorithm detects a collision with an object of the virtual environment. Depending upon the surface stiffness and structure of object, the algorithm calculates the collision force. The velocity of the tip is used for stabilizing the control and simulating the viscous friction. The calculated force is then converted to motor torque through the Jacobian matrix (4) and limited to prevent high exertion forces—to avoid any possible injury. The equation of the physical model being

$$\boldsymbol{\tau} = \mathbf{J}_A^T(\varphi)\mathbf{f}(\mathbf{p}, \dot{\mathbf{p}}) + \mathbf{n}(\varphi, \dot{\varphi}) \quad (6)$$

where $\mathbf{n}(\varphi, \dot{\varphi})$ represents linear compensation of the gravity and Coriolis contributions from (5).

C. Application of HIFE

Along with the haptic interface, a complete application for therapists has been developed. The application database enables patient selection from a list of recorded patients with patient data, experiment level setting, and the size of the patient workspace recorded last. A number of different experiment types and levels of complexity for each type, which can easily be selected, were implemented.

Therapists can select between single experiment mode and experiment list mode. In the former case, particular parameters can be set separately for each experiment, the experiment then actuated with a click on the button. According to the list mode, application is performed by running preset list of experiments and parameters with a click on the list button. Further details regarding the list are described in Section II-D.

Within the application, the output force is limited to the program value specified by the user. Soft start of exercise is implemented in order to eliminate unforeseen movement of the haptic device at the beginning of exercise. These movements could

occur due to the nature of some experiments, e.g., the “Spring Move” experiment, which calculates a high output force at the beginning, provided the fingertip is away from the center point. The output force increases linearly within the first 2 s from zero to the desired value.

All experiments are implemented within a virtual room with virtual walls and experimental objects placed in the space. MAVERIK—a VR micro-kernel system [32]—has been used for graphic visualization. A virtual ball represents the device tip, i.e., the fingertip. The color of the ball changes from red to green at the beginning of an experiment, it reverting to red on stopping thereof. The patient has 2 s to recognize a new scene before the next experiment starts.

D. Experiments

1) *Workspace Capture*: Before working with a new patient, when the hand or patient himself have been changed, the workspace of finger must be defined. Depending upon the relative position and size of the workspace, objects therein are placed according to their size and center position. The relative positions of the objects are predefined for each experiment setup and level. The graphic presentation of the experiments is shown in Fig. 4.

2) *“Static Test” Experiment*: The “Static Test” experiment is focused on evaluation of maximal static finger forces at the tip in different postures and orientations. The patient moves the finger as far as possible along each direction of the tunnel. The program generates narrow tunnels between two predefined points. The force linearly increases along the tunnel direction as a virtual spring extension. The spring constant and the number of tunnels increase with the higher levels of the experiment. Thus, mainly maximal forces of finger extension and flexion are evaluated.

3) *“Buttons” Experiment*: In this experiment, the coordination of finger movement and the contact force are evaluated. The exerted force depends upon the button position within the finger workspace. The patient presses the virtual buttons as hard as possible. Buttons are placed all over the finger workspace. Each button moves down, and the color changes when pressed from the top. The button stiffness and the number of buttons increase, and the contact area decreases with higher experiment levels.

4) *“Jo Ball” Experiment*: The simplest experiment has a ball attached to a finger via a virtual spring. Voluntary finger movement is encouraged by haptic information, i.e., the patient can feel the interaction and the collisions with the ball. The patient is instructed to move the ball as fast as possible. The velocity of fingertip movement and the wrapped area of the trajectory are key parameters of the experiment.

5) *“Tunnel” Experiment*: In this experiment, the patient has to follow the centerline of the tunnel from the entrance to the end. At moving the fingertip away from the centerline, the tunnel wall still holds the fingertip inside. The aim of this experiment is to advance with as few collisions with the wall as possible. The second goal is to follow the tracking ball, which moves along the centerline with a predefined velocity. The tunnel complexity and the tracking velocity increase with higher experiment levels.

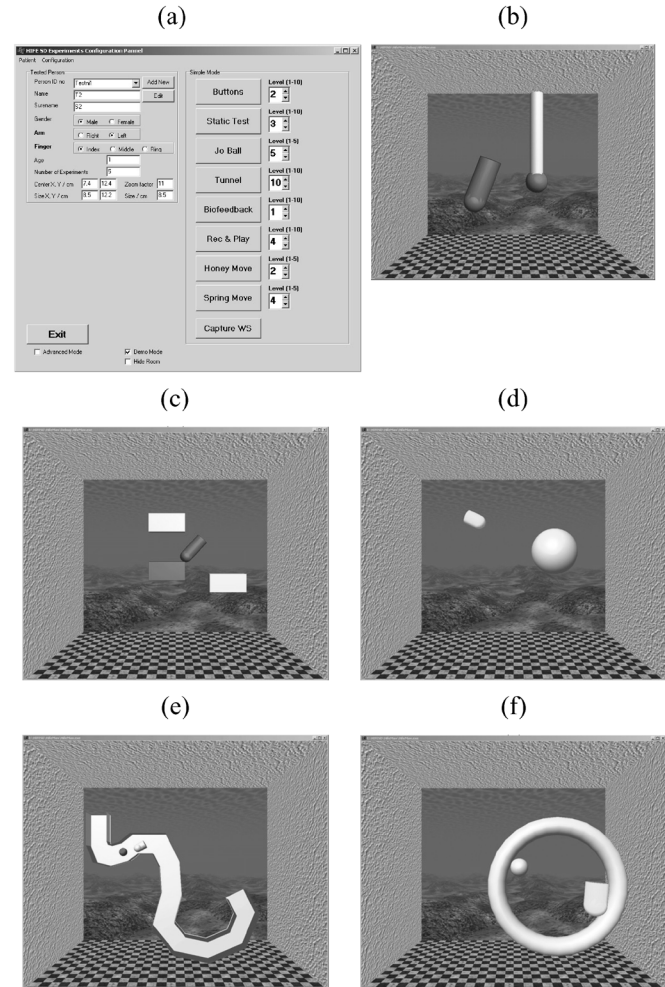


Fig. 4. (a) Application GUI and virtual experiments for (b) “Static Test,” (c) “Buttons,” (d) “Jo Ball,” (e) “Tunnel,” and (f) “Spring Move” experiments. Room consists of virtual walls and experimental objects placed within same. Virtual finger is composed of virtual ball and cylinder.

The deviation from the centerline and the accuracy of following the tracking ball are key parameters of the experiment.

6) *“Spring Move” Experiment*: The patient exercises a finger by stretching a virtual spring. The spring is visualized as a torus with one side attached to the center of the finger workspace, the other side attached to the fingertip. The force increases linearly when extending the spring. The spring constant increases with higher levels of the experiment. The velocity of the fingertip movement, the stretching forces, and the wrapped area of the trajectory are key parameters of the experiment.

7) *Experiment List*: At the beginning of testing, the patient proceeds individually through each experiment. This serves as an introduction to experiments and for determination of experiment level. Based on levels of experiments, an experiment list is generated, which consists of “Static Test,” “Buttons,” “Jo Ball,” the “Tunnel” and “Spring Move” experiment. As to duration, experiments are limited to sixty seconds, with the exception of “Static” and “Tunnel” tests, where the experiment is finished after all the objects have been evaluated or the end of the tunnel has been reached.

E. Data Analysis

In the statistical analysis, all recorded data was processed with MATLAB software. Recorded data was sampled at a frequency of 100 Hz, and patient data as well as the experiment setup for each experiment were stored in a text file. The position, the velocity, and the force signals were filtered in real time with a second-order Butterworth filter having a cutoff frequency of 40 Hz. The relevant parameters were calculated for each participant, and for each experiment, and were stored in a “MySQL” database for easier further processing. Three relevant parameters p_n , objects of analysis, are presented in the following sections. These are as follows:

- $\bar{v}[cm/s]$: mean value of fingertip velocity ($p_n = v_n$);
- $\bar{F}[N]$: mean value of the exerted force ($p_n = F_n$);
- wrapped area WA[cm^2]: size of the area of fingertip movement.

The mean value of the i th relevant parameter \bar{p}_i and the successive number of type of experiment $se\#$ for a patient, marked with a patient ID, were calculated as

$$\bar{p}_i = \frac{1}{N} \sum_{n=1}^N p_n \quad (7)$$

where $e\#$ is the experiment number, N is the number of all samples in the experiment, and p_n is the n th sample of the relevant experiment parameter.

F. Statistical Analysis

The least square regression line [33] utilizing a logarithmic function was used to mathematically describe the progress of relevant parameters ${}^{ID}\mathbf{p}_i = [{}^1_{ID}\bar{p}_i, {}^2_{ID}\bar{p}_i, \dots, {}^m_{ID}\bar{p}_i]^T$ where m is the number of experiments. Equation (8) specifies the regression line ${}^{ID}\mathbf{p}_{i,reg}$ function

$${}^{ID}\mathbf{p}_{i,reg} = a \log({}^{ID}\mathbf{p}_i) + b, \quad (8)$$

where \mathbf{p}_i represents the vector of the mean values for each successive experiment, a being the progression coefficient, and b representing the offset of the line.

To calculate parameters a and b the input function has first been defined as follows:

$$\mathbf{U} = [\log({}^{ID}\mathbf{p}_i), \mathbf{1}_{m \times 1}]_{m \times 2} \quad (9)$$

where m represents the length of vector ${}^{ID}\mathbf{p}_i$. The parameters a and b as vector \mathbf{k} were calculated using the following equation:

$$\mathbf{k} = [(\mathbf{U}^T \mathbf{U})^{-1} \mathbf{U}^T {}^{ID}\mathbf{p}_{i,reg}]_{2 \times 1} = [a, b]^T. \quad (10)$$

An example of the regression line for the wrapped area WA parameter at the “Jo Ball” experiment is presented in Fig. 5. Each dot represents an experimental mean value, and solid and dashed lines represent the calculated regression line and the mean value, respectively.

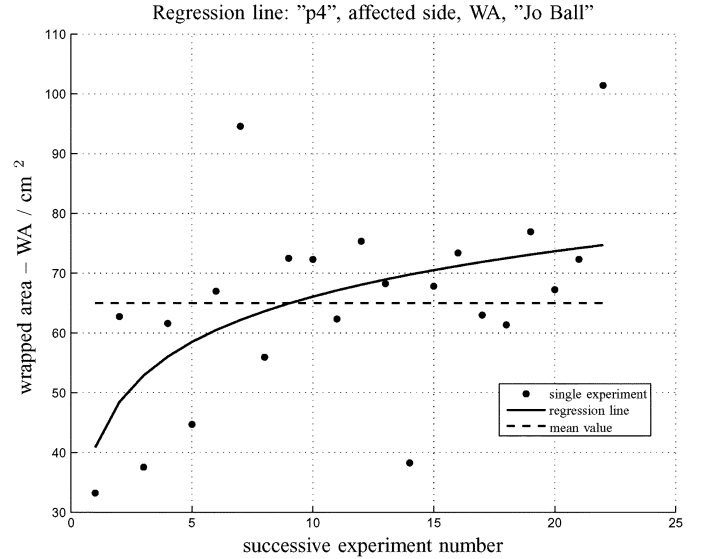


Fig. 5. Regression line for wrapped area of the “Jo Ball” experiment for patient “p4”.

G. Typical Fingertip Traces

Traces for “Jo Ball” and “Spring Move” experiments are presented in Fig. 6. For the “Jo Ball” experiment, the traces are more condensed on the left side, i.e., the finger is extended most of the time and the MCP joint is mostly moved. The traces define a larger area than on the right side since the finger is not loaded with a spring force. On the right side of Fig. 6 the traces for “Spring Move” are condensed on a line from the center point to the point where the finger is fully extended and to the point where the finger is fully flexed.

H. Participants

A total of nine patients (three women, men; aged six between 25 and 75 years) with neuromuscular diseases participated in the present study. The patients suffered from ischemic or hemorrhagic stroke. Table I presents a list of patients and the results of the therapist assessment on the functional independence measure (FIM) scale [34], [35]. Actually, only the motor component of the functional independence measure (M-FIM) scale is presented. In the second column of Table I patient details are provided. These details include age, gender (M/F), affected hand side (L/R), measured finger [index (I), middle (M)], type of stroke (Ishem-ischemic, Hemo-hemorrhagic), and duration of disability. The third column gives a value of the M-FIM index at discharge of patient, the last column presenting the improvement in the M-FIM index from admission to discharge. The control group consisted of five healthy male volunteers aged between 23 and 29 years. All participants were informed of the test procedures, and have given their consent to participate therein.

I. Experimental Protocol

The affected hand side of patients was assessed every day during a one-month period of therapy, the nonaffected side having been controlled once a week. Both hands of the healthy

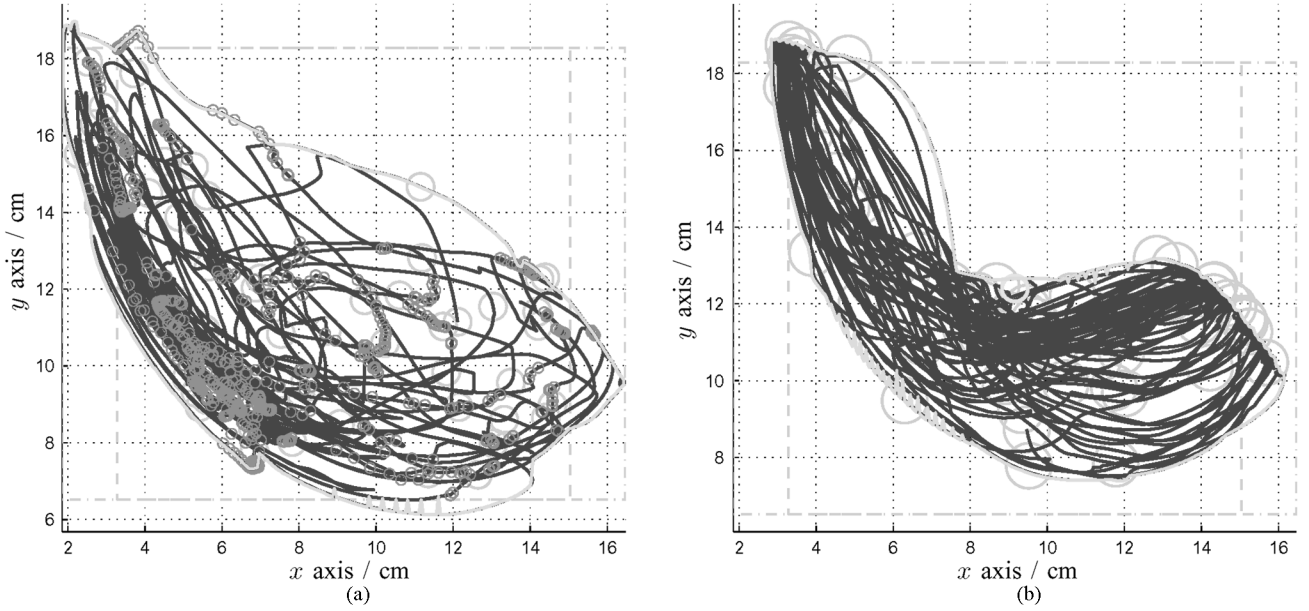


Fig. 6. Typical finger tip path for (a) "Jo Ball" and (b) "Spring Move" experiments.

TABLE I
PATIENT DATA AND FIM CLINICAL SCALE RESULTS

pat.No	patient data (age, sex, aff. side, finger, type, duration)	M-FIM (discharge)	Δ M-FIM
p1	50, M, L, I, Ishem, 5.5	77	2
p2	62, F, R, I, Hemo, 1.5	68	19
p3	62, F, R, M, Hemo, 1	71	25
p4	20, M, R, M, Hemo, 1	72	15
p5	64, M, L, I, Ishem, 3	74	4
p6	66, M, L, M, Ishem, 8	59	1
p7	74, M, R, M, Ishem, 3	73	2
p8	63, F, L, I, Hemo, 3.5	73	2
p9	64, M, R, I, Ishem, 7	79	1

volunteers were evaluated for one week on a daily basis. All the participants were given the same instructions for each experiment. At first, the finger workspace was measured and the experiment list (Section II-D7) was evaluated. Each completed experiment list per day per finger lasted between six and seven minutes.

During the tests, the participants were sitting in a chair in front of the computer screen beside the haptic device. The forearm was secured in a wooden hand rest and firmly attached with straps. The elbow was positioned at an angle of 90° of flexion, and the shoulder was in neutral position. The therapist monitored the patient hand test posture to prevent unexpected motion of hand.

III. RESULTS AND DISCUSSION

In the following section, statistical results of experiments are presented. The figures include statistics for both hand sides of patients, as well as those of healthy subjects.

The mean value of the exerted force \bar{F} for "Spring Move" during a particular experiment trial was calculated first. In this experiment, the forces were exerted for the whole duration of the experiment in dependence upon the distance between the

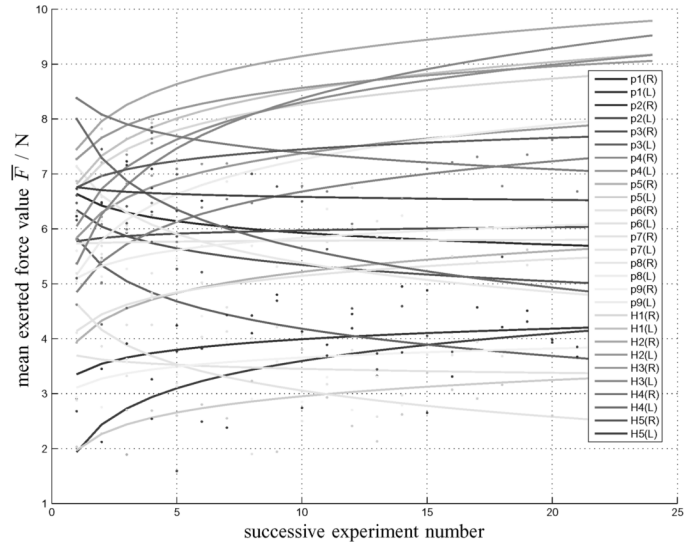


Fig. 7. Regression lines for the mean exerted force value \bar{F} versus successive experiment number. Lines are calculated using the least square error method with logarithmic fitting.

fingertip and the center point. The mean values (vertical) versus the successive experiment number of each participant are presented in Fig. 7 as dots. Furthermore, regression lines are calculated and plotted as solid lines in the same figure. The least square error method with logarithmic fitting as described earlier was used for calculating the coefficients of lines. An upward tendency of the lines can be noticed for almost all patients. The values for the healthy participants are above the patient lines.

Fig. 8(a) presents the coefficients of the regression lines from Fig. 7. The x axis shows the progress coefficient, while the y axis shows the mean value of all experiments \bar{F} [(cf. (8)).

It can be observed that:

- 1) the progress coefficients of the affected hand side of patients are higher than those of the nonaffected side;

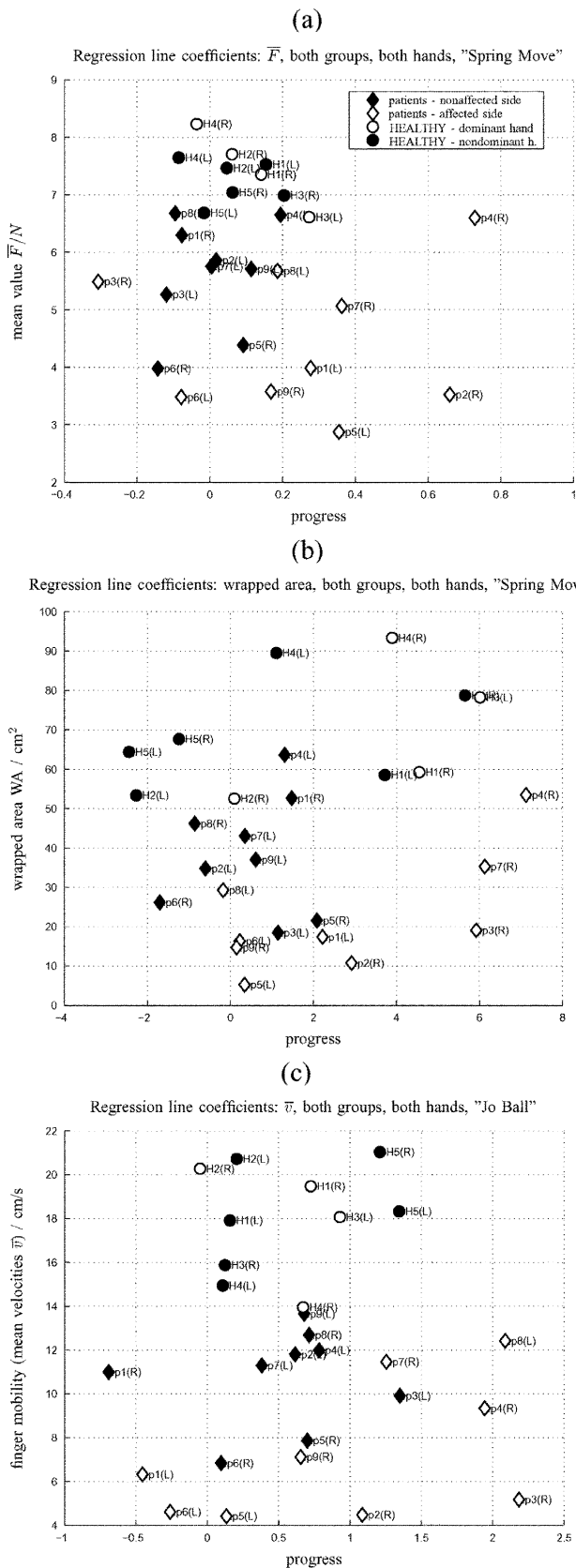


Fig. 8. (a) Regression line coefficients for the lines of Fig. 7. (b) Coefficients of regression lines valid for wrapped area size in "Spring Move" experiment. (c) Coefficients of regression lines for finger mobility (mean velocities) in the "Jo Ball" experiment. Here, the following symbols are used: \diamond —patient affected hand side; \blacklozenge —patient nonaffected hand side; \circ —healthy dominant hand side; \bullet —healthy nondominant hand side.

- 2) the mean values of the exerted forces of the nonaffected side of patients are higher than those of the affected side;
- 3) the mean values of the exerted forces of patients are lower than the exerted forces of healthy volunteers;
- 4) the progress coefficients and the mean values of either hands of healthy volunteers are very similar.

Furthermore, we would like to present the results for wrapped area WA in similar manner. We assume that the area covered during the motion correlates with the range of motion—ROM—of the finger since the finger is not loaded. The person is only visually and haptically motivated. The size depends individually upon the phalange dimensions, however, progress can still be an important messenger. The results for ROM coefficients are depicted in Fig. 8(b). The findings are similar as in the previous example of mean exerted forces. The progress line parameters for static values (mean exerted forces) seem to correlate very well with the ROM parameters.

Moreover, in the same experiment mean velocities can be observed as a parameter reflecting mobility, according to presentation in Fig. 8(c). More progress for the patient affected hand sides can be encountered here as also seen in the previous Figures. On the contrary, the progress coefficients and the mean values for the dominant hand side both appear to be higher at the majority of the healthy volunteers.

ROM values for both experiments are next compared in Fig. 9(a). In "Jo Ball" the finger is free to move, while in "Spring Move" the finger is loaded, i.e., it must exert some force. The most interesting observation is that ROMs are almost independent of the loading of the finger. This can be claimed after it had been established that the bullets in Fig. 9(a) are grouped along a linear slope. If the values were clustered in one or several groups of points outside the linear slope, the wrapped area would be dependent upon the type of experiment, the contact force, or other parameters.

Fig. 9(b) addresses the question of improvement (change) in ROM as well as improvement in force generation capability. Higher progress values can be observed for patients (marked with diamonds) in the "Spring Move" experiment, i.e., finger strength increases more than ROM during therapy. Healthy subjects are located close to zero progress for both cases with only minor deviations.

The kinematic to static data comparison in Fig. 9(c) shows strength and mobility progress. The results deviate slightly. According to Fig. 9(c), in some cases mobility progress overtakes strength progress, while in other cases the opposite is true. Values for the healthy subjects, marked as circles, are located close to zero progress and deviate slightly in both cases.

When compared to the given M-FIM scale data of Table I, the results according to the present study are very well correlated. When patients with higher progress values on the M-FIM scale are considered, the following can be noticed: For example, patient "p3" showed great progress in ROM and mobility values (Figs. 8(b) and (c), and Table I), while the force exerted decreased during therapy (Fig. 8(a)). Patient "p2" also showed more progress in exerted force value, while less progress, but still some, can be observed on other two values. Similar conclusions can be drawn from comparisons in other subjects.

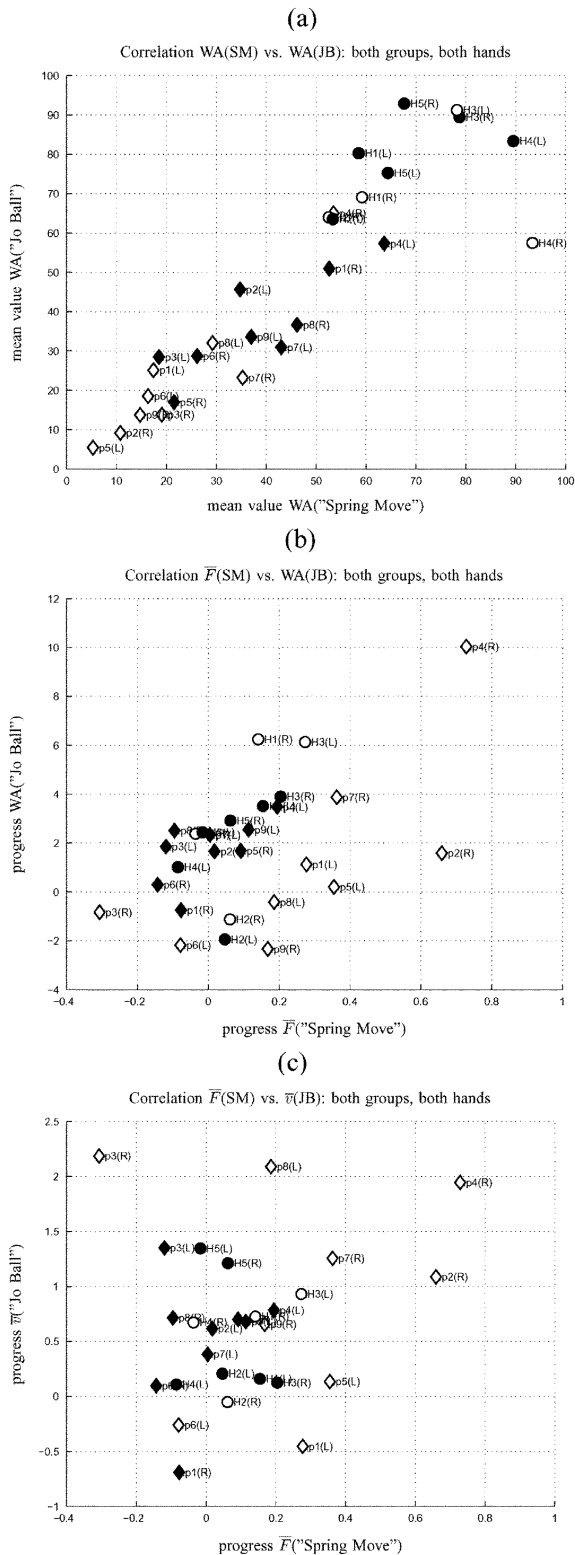


Fig. 9. (a) Comparison of the wrap ROMs at “Spring Move” and “Jo Ball” experiments. “Spring Move” experiment represents a loaded finger situation, while “Jo Ball” offers movement not loaded. (b) Comparison of finger strength and ROM progress. (c) Comparison of finger strength and mobility.

IV. CONCLUSION

This paper presents a newly developed haptic device and its application for finger exercise and assessment. Five different

types of exercises were implemented in a virtual environment. The device was evaluated in a group of patients after stroke and during a one-month period of therapy. The selection of exercises was found to be suitable for the finger and assessing the functionality in patients with neuromuscular diseases. Analysis of experiments and observations are presented in this paper. Only two types of experiments are presented in detail due to the limited paper length and for intelligible presentation of the results. Our observation is that progress during therapy of the affected hand side in patients is better than the one of the nonaffected side. As expected, the mean values for kinematic and static parameters in patients are found to be lower than for healthy volunteers. We also verified that the progress coefficients and the mean values for either hands of healthy volunteers are very similar. Results from the present study were compared to the M-FIM scale and are very well correlated. Great correlation to the existing clinical scale that was observed makes application suitable for objective assessment of post-stroke disability.

Application as presented can further be improved by upgrading the haptic interface to exercise more than one finger at a time. In summary, the haptic device, along with the virtual environment, performed well, while experiments as selected proved to be suitable for the population with neuromuscular diseases.

ACKNOWLEDGMENT

The authors would like to thank the patients and volunteers who participated in the study, and to occupational therapists D. Breclj, M. Javh, J. Poje, and S. Kotnik, Institute for Rehabilitation, Republic of Slovenia.

REFERENCES

- [1] J. Hermsdörfer, E. Hagl, D. Nowak, and C. Marquardt, “Grip force control during object manipulation in cerebral stroke,” *Clin. Neurophysiol.*, vol. 114, no. 5, pp. 915–929, 2003.
- [2] T. Iberall, “Human prehension and dextrous robot hands,” *Int. J. Robot. Res.*, vol. 16, no. 3, pp. 285–299, Jun. 1997.
- [3] S. Li, M. Latash, G. Yue, V. Siemionow, and V. Sahgal, “The effects of stroke and age on finger interaction in multi-finger force production tasks,” *Clin. Neurophysiol.*, vol. 114, no. 9, pp. 1646–1655, 2003.
- [4] S. McPhee, “Functional hand evaluations: A review,” *Amer. J. Occup. Ther.*, pp. 158–163, 1987.
- [5] F. Valero-Cuevas, “An integrative approach to the biomechanical function and neuromuscular control of the fingers,” *J. Biomech.*, vol. 38, no. 4, pp. 673–84, 2005.
- [6] F. Valero-Cuevas, N. Smaby, M. Venkadesan, M. Peterson, and T. Wright, “The strength-dexterity test as a measure of dynamic pinch performance,” *J. Biomech.*, vol. 36, no. 2, pp. 265–270, 2003.
- [7] F. Valero-Cuevas, “Applying principles of robotics to understand the biomechanics, neuromuscular control and clinical rehabilitation of human digits,” in *Proc. 2000 IEEE Int. Conf. Robot. Automat.*, 2000, pp. 255–262.
- [8] W. Greenleaf and T. Piantanida, J. D. Bronzino, Ed., “Medical applications of virtual reality technology,” in *The Biomedical Engineering Handbook*, 2nd ed. Boca Raton, FL: CRC, 2000, vol. II.
- [9] V. Popescu, G. Burdea, M. Bouzit, and V. Hentz, “A virtual-reality-based telerehabilitation system with force feedback,” *IEEE Trans. Inf. Technol. Biomed.*, vol. 4, no. 1, pp. 45–51, Mar. 2000.
- [10] R. Teasell and L. Kalra, “What’s new in stroke rehabilitation,” *Stroke*, vol. 35, pp. 383–385, Feb. 2004.
- [11] J. Deutsch, J. Latonio, G. Burdea, and R. Boian, “Post-Stroke Rehabilitation with the Rutgers Ankle System—A Case Study,” *Presence*, vol. 10, no. 4, pp. 416–430, 2001.

- [12] W. Harwin, R. Loureiro, F. Amirabdollahian, M. Taylor, G. Johnson, E. Stokes, S. Coote, M. Topping, C. Collin, S. Tamparis, J. Kontoulis, M. Muni, P. Hawkins, and B. Driessen, C. Marincek, Ed., "The gentle/s project: A new method for delivering neuro-rehabilitation," in *Assistive Technology—Added Value to the Quality of Life AAATE'01*. Amsterdam, The Netherlands: IOS Press, 2001, pp. 36–41.
- [13] G. Burdea, "Virtual rehabilitation—Benefits and challenges," *Methods Inf. Med.*, vol. 42, pp. 519–523, 2003.
- [14] D. Jack, R. Boian, A. Merians, M. Tremaine, G. Burdea, S. Adamovich, M. Recce, and H. Poizner, "Virtual reality-enhanced stroke rehabilitation," *IEEE Trans. Neural Syst. Rehabil. Eng.*, vol. 9, no. 03, pp. 308–318, Sep. 2001.
- [15] R. Jones, "Measurement of sensory-motor control performance capacities: Tracking tasks," in *The Biomedical Engineering Handbook*, J. D. Bronzino, Ed., 2nd ed. Boca Raton, FL: CRCs, 2000, vol. II.
- [16] A. Bardorfer, M. Muni, A. Zupan, and A. Primozic, "Upper limb motion analysis using haptic interface," *IEEE/ASME Trans. Mechatron.*, vol. 6, pp. 253–260, 2001.
- [17] G. Byers, B. Goldstein, and J. Sanders, "An electromechanical testing device for assessment of hand motor function," *IEEE Trans. Rehabil. Eng.*, vol. 6, no. 1, pp. 88–94, Mar. 1998.
- [18] K. Kilgore, R. Lauer, and P. Peckham, *IEEE Trans. Rehabil. Eng.*, vol. 6, no. 4, pp. 424–429, Dec. 1998.
- [19] Z. Li and R. Goitz, "Biomechanical evaluation of the motor function of the thumb," *Technol. Health Care*, vol. 11, no. 4, pp. 233–43, 2003.
- [20] G. Kurillo, T. Bajd, and R. Kamnik, "Static analysis of nippers pinch," *Neuromodulation*, vol. 6, pp. 166–175, 2003.
- [21] G. Kurillo, A. Zupan, and T. Bajd, "Force tracking system for the assessment of grip force control in patients with neuromuscular diseases," in *Clin. Biomech.*, Bristol, U.K., Dec. 2004, vol. 19, no. 10, pp. 1014–21.
- [22] D. Kamper and W. Rymer, "Impairment of voluntary control of finger motion following stroke: Role of inappropriate muscle coactivation," *Muscle & Nerve*, vol. 24, pp. 673–81, 2001.
- [23] T. H. Massie and J. K. Salisbury, "The {PHANToM} haptic interface: A device for probing virtual objects," presented at the Proc. ASME Winter Annu. Meeting Symp. Haptic Interfaces Virtual Environ. Teleoperator Syst., Chicago, IL, Nov. 1994.
- [24] PHANToM SensAble Technologies Woburn, MA [Online]. Available: http://www.sensable.com/products/phantom_ghost/phantom.asp
- [25] M. Turner, D. Gomez, M. Tremblay, and M. Cutkosky, "Preliminary tests of an arm-grounded haptic feedback device in telemanipulation," in *Proc. ASME IMECE 7th Annu. Symp. Haptic Interfaces*, Anaheim, CA, 1998, vol. DSC-64, pp. 145–149.
- [26] M. Bouzit, G. Burdea, G. Popescu, and R. Boian, "The rutgers master ii-new design force-feedback glove," *IEEE/ASME Trans. Mechatron.*, vol. 7, no. 2, pp. 256–263, Jun. 2002.
- [27] G. Burdea, *Force and Touch Feedback for Virtual Reality*. New York: Wiley, 1996.
- [28] U. Mali and M. Muni, "HIFE-haptic interface for finger exercise," *IEEE/ASME Trans. Mechatron.*, vol. 11, no. 1, pp. 93–102, Feb. 2006.
- [29] U. Mali and M. Muni, "Real-time control of haptic device using personal computer," in *IEEE Region 8 EUROCON 2003: Computer as a Tool*, Ljubljana, Slovenia, Sep. 2003, vol. 1, pp. 401–404.
- [30] B. Buchholz, T. Armstrong, and S. Goldstein, "Anthropometric data for describing the kinematics of the human hand," *Ergonomics*, vol. 35, no. 3, pp. 261–73, 1992.
- [31] L. Sciavicco and B. Siciliano, *Modelling and Control of Robot Manipulators*, 2nd ed. London, U.K.: Springer-Verlag, 2000.
- [32] MAVERIK—A VR micro kernel, [Online]. Available: <http://www.gnu.org/software/maverik/maverik.html>, Online. Available
- [33] S. Chapra and R. Canale, *Numerical Methods for Engineers*, 2nd ed. New York: McGraw-Hill, 1988.
- [34] K. J. Ottenbacher, Y. Hsu, C. V. Granger, and R. C. Fiedler, "The reliability of the functional independence measure: A quantitative review," *Arch. Phys. Med. Rehabil.*, vol. 77, no. 12, pp. 1226–32, 1996.

- [35] M. E. Cohen and R. J. Marino, "The tools of disability outcomes research functional status measures," *Arch. Phys. Med. Rehabil.*, vol. 81, no. 12, pp. S21–29, Dec. 2000, S2.



Uroš Mali received the B.Sc. and M.Sc. degrees in electrical engineering, in 2000 and 2003, respectively, from the Faculty of Electrical Engineering, University of Ljubljana, Slovenia, where he is currently working toward the Ph.D. degree.

In 1999, he was with the Dynamical Systems and Control Laboratory, The Johns Hopkins University, Baltimore, MD. He is currently an Assistant with the Laboratory of Robotics and Biomedical Engineering, Faculty of Electrical Engineering, University of Ljubljana. His research interests include

design, construction and real-time control of haptic devices and robots for virtual reality supported hand and finger rehabilitation.



Nika Goljar received the M.D. degree from the University of Ljubljana, Slovenia, in 1987, the M.Sc. degree from University of Zagreb, Croatia, in 1992, and the D.Sc. degree from University of Ljubljana, Slovenia in 1999.

Her research interests were focused in functional reorganization of the somatosensory system in stroke patients, enhancement of hemiplegic patients rehabilitation by means of functional electrical stimulation, and outcome measurement of stroke rehabilitation.

She became a resident in physical medicine and rehabilitation in Rehabilitation Institute Ljubljana, Slovenia, in 1990 and was qualified as a specialist of physical medicine and rehabilitation in 1994 from Medical School Ljubljana, University of Ljubljana, Slovenia. From 1997, she was Teaching Assistant for physical medicine and rehabilitation at Medical School Ljubljana. Currently, she is Head of Stroke rehabilitation unit in Rehabilitation Institute Ljubljana, Slovenia.

Dr. Goljar is member of European Board of Physical and Rehabilitation Medicine.



Marko Muni (M'88) received the B.Sc., M.Sc., and D.Sc. degrees in electrical engineering from the University of Ljubljana, Slovenia, in 1986, 1989 and 1993, respectively.

His research interests were focused in functional electrical stimulation of paraplegic lower extremities with surface electrode systems, including measurements, control, biomechanics, and electrical circuits. From 1989, he was Teaching Assistant and from 1997 Assistant Professor at the Faculty of Electrical Engineering, Ljubljana, Slovenia. From 1995 to 1996, he was a Research Assistant with the Implanted Devices Group, Department of Medical Physics and Bioengineering, University College London, London, U.K., and Royal National Orthopaedic Hospital Trust, Stanmore, U.K. In the last period, his interest is focused on robot contact with environment and use of haptic interfaces in the field of rehabilitation engineering (projects GENTLE/S, I-Match, Alladin).

Dr. Muni is recipient of the Zois award in 2002, given for outstanding scientific contributions by the Slovene Ministry of Science, Education and Sport. Currently, he is Professor and Head of Laboratory of Robotics and Biomedical Engineering at the Faculty of Electrical Engineering, Ljubljana, Slovenia. He is member of the IFMBE, IFESS, and IFAC.